ELSEVIER

Biochimica et Biophysica Acta 1420 (1999) 73–85

BIOCHIMICA ET BIOPHYSICA ACTA
BBA

www.elsevier.com/locate/bba

Fluorescence, absorption and electron spin resonance study of bacteriochlorin *a* incorporation into membrane models

Maryse Hoebeke [a,*], Xavier Damoiseau [a], Hans J. Schuitmaker [b], Albert Van de Vorst [a]

[a] *Department of Experimental Physics, Institute of Physics B5, University of Liège, 4000 Liège, Belgium*
[b] *Department of Ophthalmology, State University of Leiden, Leiden, Netherlands*

Received 26 November 1998; received in revised form 12 May 1999; accepted 27 May 1999

Abstract

Analysis of the bacteriochlorin *a* absorption spectra suggests the existence of a monomer–dimer equilibrium, particularly intense in phosphate buffer and favored by a decrease of the pH. The dye in methanolic solution is predominantly in monomeric form. Fluorescence and electron spin resonance nitroxide spin labeling measurements indicate that incorporation into the lipid phase of dimyristoyl-L-α-phosphatidylcholine liposomes induces dye monomerization. Moreover, the molecules are bound in the external surface of the vesicles and a complete incorporation is ensured by a lipid-to-dye ratio greater than 125.

Keywords: Bacteriochlorin *a*; Liposome; Fluorescence; Absorption; Electron spin resonance; Spin labeling

1. Introduction

Bacteriochlorin *a* (BCA) is attracting considerable attention in view of its potential use in light-induced process as photodynamic therapy (PDT) which is an innovative modality for the treatment of small and superficial tumors [1]. Indeed, particular attention is devoted to sensitizers presenting a tumor cell preferential retention and absorbing above 600 nm. In this spectral region, endogenous tissular components are transparent to the incident radiation, minimizing the risk of photodamage at the level of cells or tissues not containing the photosensitizers. Moreover, under light irradiation, these dyes must produce active oxygen species able to react with the surrounding biological components inducing lethal damage. BCA answers completely to these preliminary requirements [2,3]. In vivo, upon illumination, BCA induces tumor necrosis through vascular and direct cellular effects [3,4]. At the dosages used to induced photodynamic effects, no adverse effects of BCA are observed in mice, rats and rabbits [3–8]. Moreover, it has been shown that BCA-PDT is able to induce non-specific systemic immune suppression [9].

Abbreviations: BCA, bacteriochlorin *a*; PDT, photodynamic therapy; DMPC, dimyristoyl-L-α-phosphatidylcholine; ESR, electron spin resonance; CTPO, 3-carbamoyl-2,2,5,5-tetramethyl-3-pyrrolin-1-yloxy (carbamoyl); 5-DSA, 2-(3-carboxypropyl)-4,4-dimethyl-2-tridecyl-3-oxazolidinyloxy; 12-DSA, 2-(10-carboxydecyl)-2-hexyl-4,4-dimethyl-3-oxazolidinyloxy; 16-DSA, 2-(14-carboxytetradecyl)-2-ethyl-4,4-dimethyl-3-oxazolidinyloxy; *n*-DSA, stearic acid spin probe; ε, extinction coefficient; C_d, dimer concentration; C_m, monomer concentration; K_d, dimerization constant; ε_m, monomer molar extinction coefficient; ε_d, dimer molar extinction coefficient

* Corresponding author. Fax: +32-43-662813.

0005-2736/99/$ – see front matter
PII: S0005-2736(99)00097-8

Our previous results concerning the BCA photodynamic activity are consistent with a mixed Type 1/Type 2 reaction process [2]. However, it is very complicated to draw conclusions on the exact mechanism which induces tumor necrosis, since during PDT, the reaction pathway strongly depends on the oxygenation within the tumor [10,11], the singlet oxygen ($^1O_2$) lifetime [12,13] in a particular environment and the stability of generated radicals [14]. Type 1 reaction processes are expected to be favored in polar media while, in contrast, Type 2 mechanisms predominate in hydrophobic environments [14,15]. So, the antitumoral activity of a sensitizer appears to be mainly governed by its solubilization inside or outside the membrane. Its primary localization in biomolecules strongly depends on its lipophilic or hydrophobic character.

In support of the considerations given above, we report in the present paper absorption and fluorescence experiments on the incorporation of BCA into liposomes of dimyristoyl-L-α-phosphatidylcholine (DMPC). Liposomes are simplified and suitable model systems allowing the study of BCA partition between the lipid bilayers and the aqueous phase [16]. Because the photosensitizing efficiency of certain dyes, like protoporphyrin or hypericin, are strongly influenced by the chemicophysical conditions of the surrounding medium and by the aggregation state of the molecule [17,18], we studied the solution behavior of BCA first in a homogeneous solvent before dealing with heterogeneous systems. Although the dye is aggregated in aqueous solutions and in methanol at high concentration, our experimental results were in favor of an incorporation of BCA as monomers into the hydrophobic bilayer of small unilamellar vesicles. The absorption and fluorescence spectra characteristic of the monomeric and dimeric forms were studied over a wide range of concentrations and the values of the dimeric equilibrium constants were estimated. The λ_{max} of the dye's visible spectrum was influenced by changes in solvent polarity or pH. Combining fluorescence and an electron spin resonance (ESR) studies, the dye-to-lipids concentration ratio range was determined in which the BCA suspension can be considered to be completely bound to liposomes. Moreover, the distribution properties of BCA inside the liposome suspension was studied using a spin label occupying the aqueous phase and a series of doxyl stearic acids with the nitroxyl radical at different depths in the lipid membrane. The kinetics of reduction indicate that BCA is preferentially located in the polar aprotic zone close to the lipid–water interface.

2. Materials and methods

2.1. Chemicals

Bacteriochlorophyll *a* was purchased from Sigma or extracted from the anaerobic photosynthetic bacterium *Rhodospirillum rubrum*. Purity of the extracted bacteriochlorophyll *a* was evaluated using thin-layer chromatography (TLC). Using an eluent of 93% methanol and 7% phosphate buffer (pH 7, 10 mM), the bacteriochlorophyll *a* yielded a single blue spot on Machery–Nagel Nano–Sil C_{18}–100 TLC plates (Düren, Germany). From this starting material, the photosensitizer bacteriochlorin *a* was obtained by saponification and acid hydrolysis of bacteriochlorophyll *a* as described previously [3]. BCA was stored under nitrogen in the dark at −20°C until use.

HPLC measurements (Fig. 1) were performed using a Microsphere C18 (3 μm) column with, as the mobile phase, 680 ml of acetonitrile and 320 ml of a solution containing acetic acid (0.5 M) and aqueous ammonia (10%). The solvent was at pH 4 and 30°C. The detector was set at 360 nm. Experiments were carried out with 0.8 ml/min flow rate, 0.05 AUFS sensitivity, 40 min run time and 20 μl of 0.03 mg BCA/ml as injected volume.

Absolute methanol and chloroform were obtained from Merck. 3-Carbamoyl-2,2,5,5-tetramethyl-3-pyrrolin-1-yloxy (carbamoyl), 2-(3-carboxypropyl)-4,4-dimethyl-2-tridecyl-3-oxazolidinyloxy (5-DSA), 2-(10-carboxydecyl)-2-hexyl-4,4-dimethyl-3-oxazolidinyloxy (12-DSA) and 2-(14-carboxytetradecyl)-2-ethyl-4,4-dimethyl-3-oxazolidinyloxy (16-DSA) were from Aldrich. Dimyristoyl-L-α-phosphatidylcholine (DMPC) was from Sigma.

2.2. Liposome preparation

DMPC (5 mg/ml) was dissolved in chloroform and the solution was evaporated under vacuum in a rotary evaporator for at least 30 min. Multilamellar

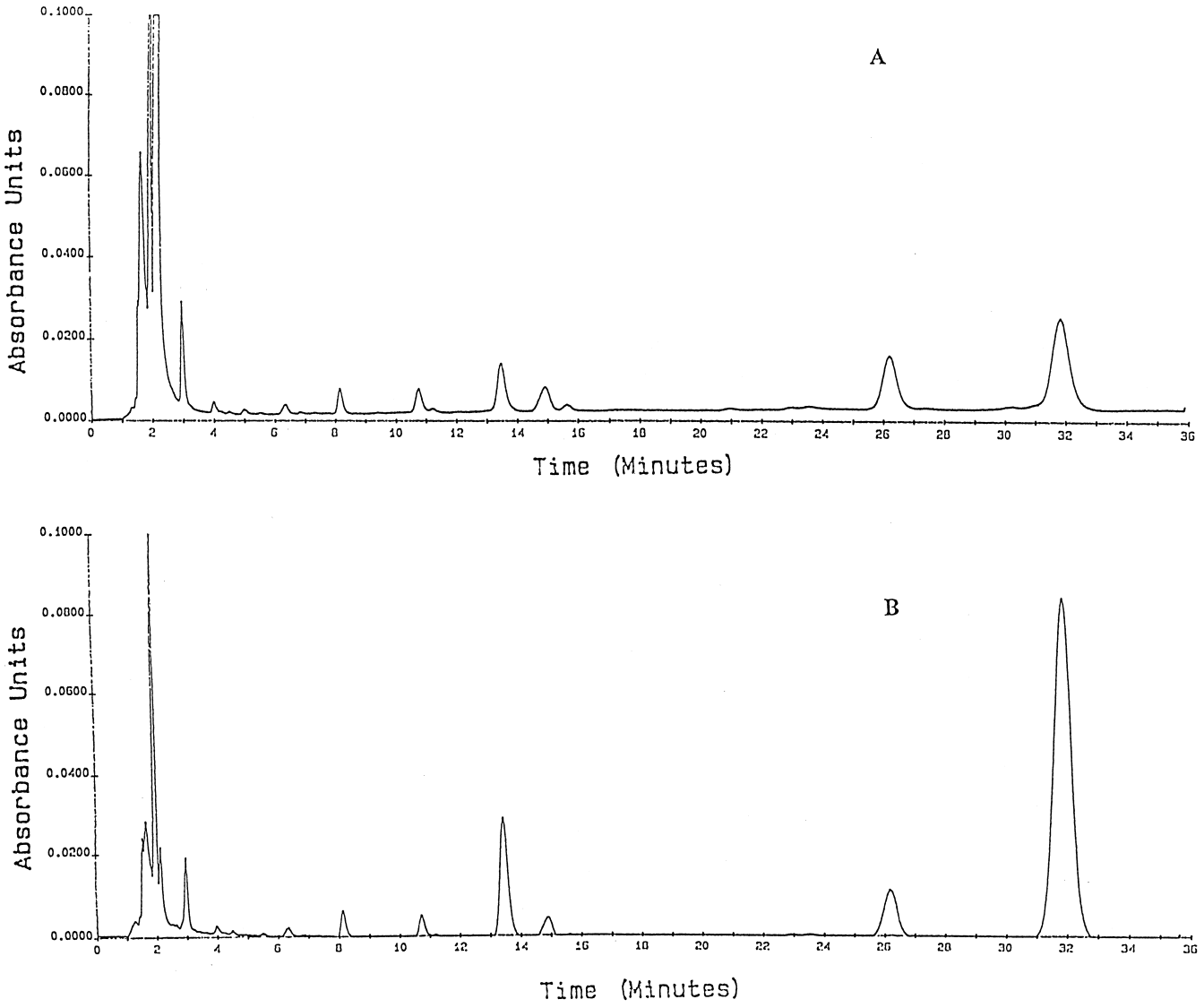

Fig. 1. HPLC analysis of (A) a freshly prepared BCA sample and (B) a BCA sample which was kept at room temperature for 75 min before injection in the system.

vesicles (MLV) were prepared by mechanical stirring (vortex mixer) of the lipid film suspended in phosphate buffer (pH 7) at a temperature above 23°C, the DMPC phase-transition temperature. Unilamellar liposomes were formed by extrusion of the MLV suspension through polycarbonate filters (0.1 μm pore size, Nucleopore, Pleasanton, CA) using a commercial extruder apparatus thermostated at a temperature above the phase-transition temperature of the phospholipids. The procedure was repeated 10 times and induced unilamellar liposomes which had a mean size of about 90 nm diameter and whose polydispersity was very low [19]. Liposomes were prepared at a lipid concentration of 7.4×10^{-3} M and then incubated for 1 h at 25°C with BCA in methanol to achieve the desired final concentration of lipids and dye. Under our experimental conditions, the final methanol concentration was 2% or less.

2.3. Fluorescence and absorption measurements

The fluorescence and absorption measurements were carried out, respectively, on an SLM-Aminco

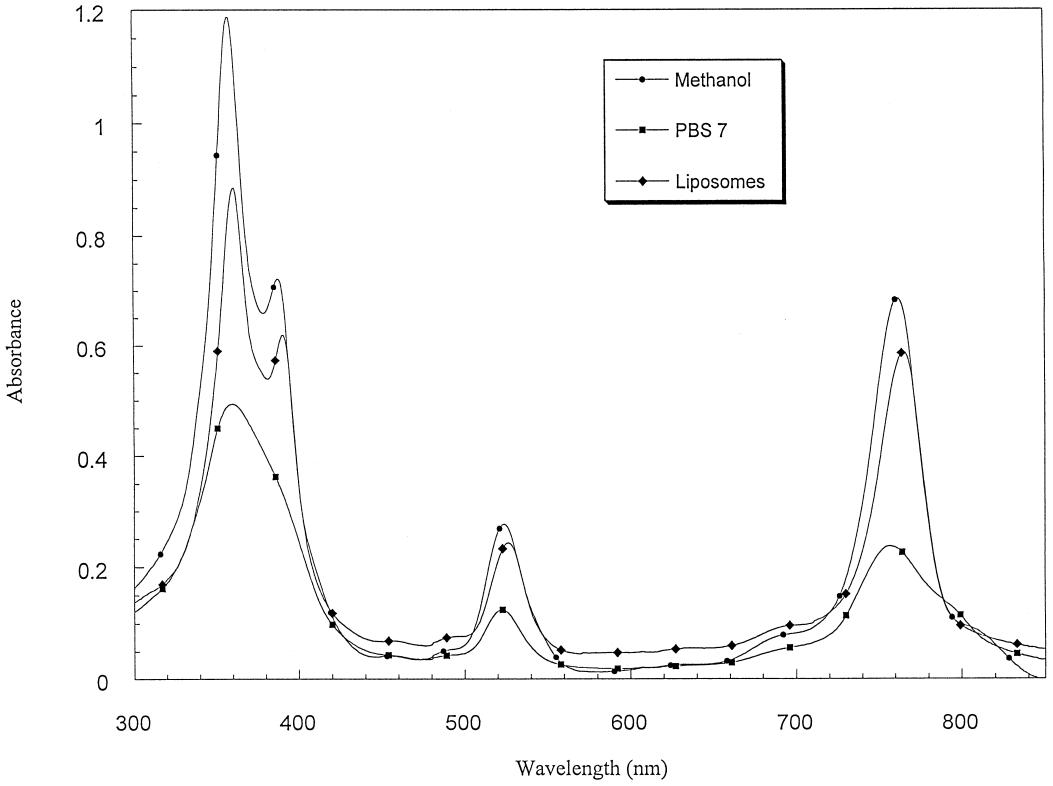

Fig. 2. Absorption spectra of BCA (1.7×10^{-5} M) in methanol, in PBS (pH 7) and incorporated into DMPC liposomes (lipid concentration 8.5×10^{-4} M).

500 spectrofluorimeter (SLM Instruments) and on a Kontron spectrophotometer (Uvikon 941 Instruments). For fluorescence measurements, 1-cm cuvettes were used; absorption measurements were performed in 0.1-, 0.2-, or 1-cm cuvettes. The temperature was controlled by circulating thermostated water through a temperature-controlled cuvette holder.

The aggregation mechanism was investigated in methanol and phosphate buffer in dependence on the dye concentration. BCA, being poorly soluble in phosphate buffer, the solutions were prepared by dilution of a methanolic stock solution. The final methanol concentration in the aqueous solution was 10%. The samples were carefully protected from light and mixed during 1 h before measuring.

2.4. *Electron spin resonance spectroscopy and spin labeling*

The lipophilic stearic acid spin labels were dissolved together with DMPC in chloroform before drying the solution under vacuum. After hydration with phosphate buffer and before extrusion, five cycles of a freeze–thawing procedure using liquid nitrogen were carried out to improve the incorporation of labeled stearic acid into the liposome phospholipid bilayer [20]. The molar ratio of label to lipid was 0.01 to assure the complete intercalation of 5-, 12- and 16-DSA in the membrane [20]. Water soluble spin label was dissolved in phosphate buffer and added to the BCA–liposome suspension.

The ESR experiments were performed at 9.56 GHz with a Bruker ESP 300E spectrometer equipped with a variable temperature controler accessory. All measurements were performed at a constant temperature above the DMPC transition temperature. Spectra were recorded by using a 50-G scan range at 20 mW microwave power and 1-G modulation amplitude.

All nitroxyl radical concentrations were calculated by double integration of the ESR spectra and calibrated against a standard solution of carbamoyl. The decrease of the signal amplitude was followed as a

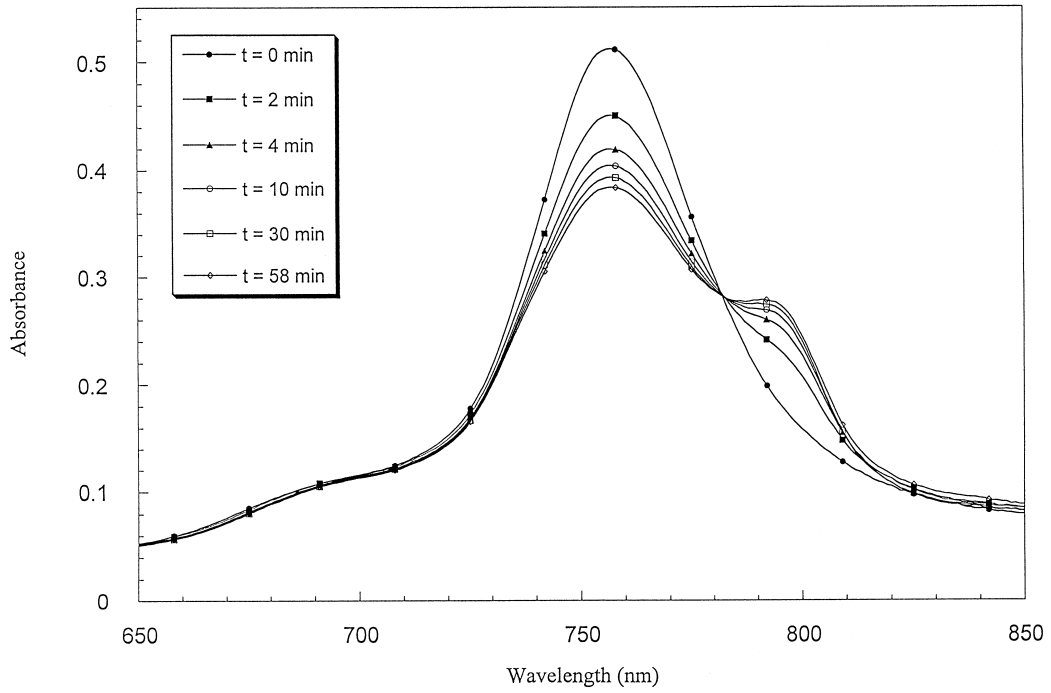

Fig. 3. Time dependence of BCA (2.5×10^{-5} M) absorption spectrum in phosphate buffer (pH 7). The spectra were recorded at 0, 2, 10, 30 and 58 min after preparing the solution.

function of the illumination time because the shape of the spectrum did not change. Nitrogen bubbling was used to eliminate oxygen from the different solutions. Samples were irradiated directly inside the microwave cavity of the spectrometer using a high pressure xenon arc lamp (XBO 150 W, Osram) and a cut-off filter eliminating light under 250 nm.

3. Results

3.1. *Effects of aggregation of BCA on its general absorption properties*

The concentration dependency of the absorption spectra of BCA in PBS and in methanol was typical of an aggregation process of the dye molecules much more extensive in polar solvent, like water, than in non-polar organic solvents [21]. At concentrations weaker than 10^{-5} M, BCA spectrum exhibited a double-band absorption peaking at approximatively $\pm$355 and 385 nm and two other peaks at $\pm$525 and 760 nm, respectively (Fig. 2). These three peaks demonstrated a slight red shift with the decrease of the dielectric constant of the solvents studied. With increasing time after the preparation of phosphate buffer solutions, the absorption spectrum of BCA showed changes leading to the development of an isobestic point (Fig. 3). These time modifications can be attributed to a change in the monomer–dimer equilibrium distribution induced by the dilution mechanism of the BCA methanolic stock solution in the phosphate buffer suspension.

In methanol, the extinction coefficient (ε) of BCA was not appreciably affected by changes in concentration in the range of 10^{-6} to 10^{-4} M (Fig. 4). Above this value and in PBS as early as at 10^{-6} M, any further increase of the dye concentration led to the attenuation of the absorption band at 525 nm, the broadening of the maximum at 355–385 and 760 nm and the formation of new bands (shoulders) at 540 and 805 nm. These shape modifications interpreted as a concentration dependence of the extinction coefficient (Fig. 4) can be attributed to an aggregation process [22], the deviations from the Beer–Lamberts' law being larger in water than in alcoholic solution as is observed for many classes of dye [17,18,23]. In PBS, the presence of one isobestic point at 782 nm (Fig. 5) reflects the existence of two various dye species, probably a monomeric

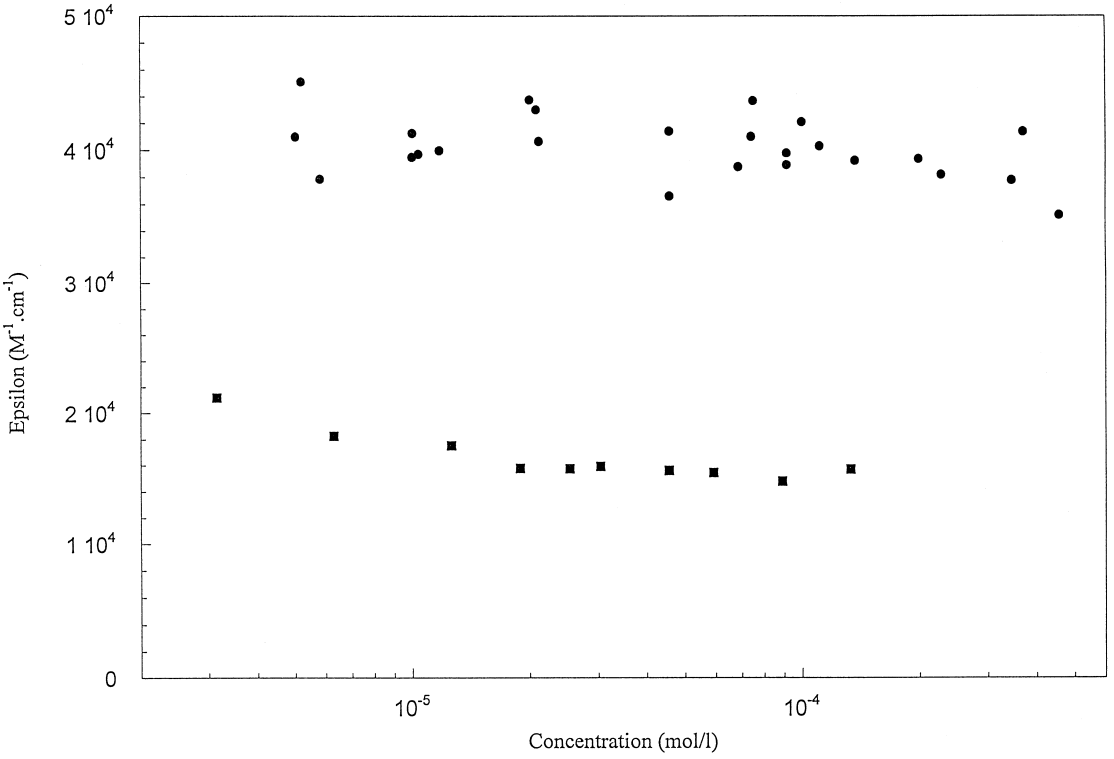

Fig. 4. Extinction coefficient as a function of BCA concentration in methanol: ■, in PBS; ●, in methanol.

and a dimeric form [24–27]. Higher aggregates were not observed in the concentration range explored. Since for BCA in PBS the aggregation process was very extensive even at a very low concentration, it was impossible for us to resolve the dye spectra in terms of pure monomeric and dimeric states. The following titration method [21,27] was thus employed to evaluate the dimerization constant K_d.

The ratio between the molar concentrations of dimers C_d and monomers C_m at equilibrium gives the values of $1/K_d$ by the law of mass action [21,23–27].

$$\frac{1}{K_d} = \frac{C_m^2}{C_d} = \frac{2\alpha^2 C_t}{(1-\alpha)} \quad (1)$$

where α is equal to C_m/C_t and $C_t = C_m + C_d$. When solving the quadratic equation of α, the following expressions are obtained.

$$2\alpha^2 C_t K_d + \alpha - 1 = 0 \quad (2)$$

$$\alpha = \frac{\sqrt{1} + 8K_d C_t - 1}{4K_d C_t} \quad (3)$$

The absorbance (Abs) being given for 1 cm optical path by

$$\text{Abs} = C_t(\varepsilon_m \alpha + \varepsilon_d \tfrac{1}{2}(1-\alpha)) \quad (4)$$

with ε_m and ε_d being the molar extinction coefficients of the monomers and dimers, respectively, the substitution of Eq. 3 in Eq. 4 allows us to write

$$\text{Abs} = \tfrac{1}{2}\varepsilon_d C_t + \frac{(\varepsilon_m - \frac{1}{2}\varepsilon_d)}{4K_d}\left(\sqrt{1} + 8K_d C_t - 1\right) \quad (5)$$

By plotting the measured ε as a function of BCA concentrations, K_d, ε_m and ε_d can thus be calculated from Eq. 5 with a curve fitting technique. K_d was found to be very high in water (Table 1).

Dimers of BCA in methanol did not appear as detectable spectral elements under 10^{-4} M dye concentration. The absence of a significant amount of dye dimers at a concentration less than 10^{-4} M and the experimental difficulties to realize absorption accurate measurements of BCA solutions at concentrations above 10^{-3} M, did not allow an exact determination of K_d an ε_d by the curve fitting technique exposed above. However, the evaluation of K_d within the restricted range of concentrations between 10^{-4}

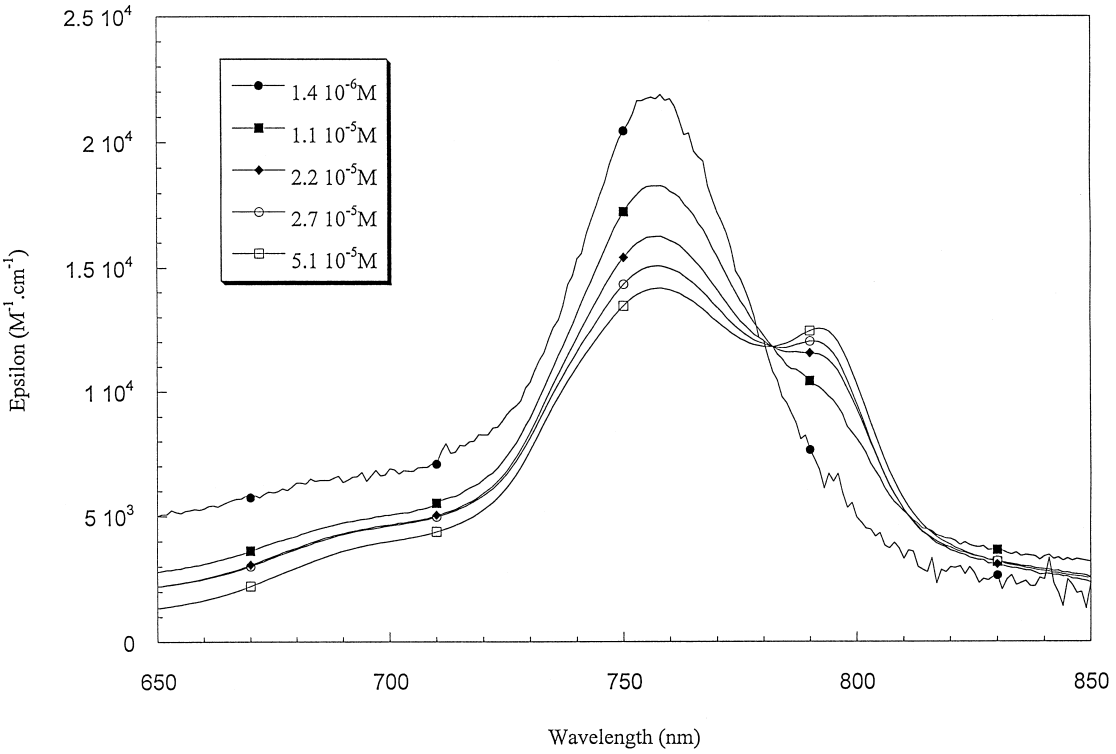

Fig. 5. Absorption spectra of BCA in PBS (pH 7) as a function of BCA concentration.

and 10^{-3} M, led to a value inferior to 1000 M^{-1}. On the basis of the above spectral considerations, the spectrum of BCA, in methanol at a concentration less than 10^{-4} M, was used as representing the monomers and the value of the corresponding ε_d is given in Table 1.

Among the various parameters which can influence the aggregation in the process, the dependence of a BCA dimerization process was examined as a function of the pH in the solution (Fig. 6). A pH decrease accelerated the establishment of the monomer–dimer equilibrium and induced a red-shift of all absorption peaks.

3.2. Binding to liposomes

Generally, the partition properties between the lipid membrane and water aqueous phase can be monitored by recording any optical change in the fluorescence or the absorption spectrum of solutions made with various lipid concentrations and a constant dye concentration [23–26]. Fig. 2 illustrates the visible absorption spectrum of BCA (1.7×10^{-5} M) in DMPC liposomes (lipid concentration 8.5×10^{-4} M). The increase of lipid concentration from 1.5×10^{-4} to 2.5×10^{-3} M for a constant dye concentration of 1.2×10^{-5} M induced mainly a regular

Table 1
BCA absorption parameters in methanol and PBS (pH 7)

	K_d (M^{-1})	ε_d (M^{-1} cm^{-1})	ε_m (M^{-1} cm^{-1})
Methanol	<1000	–	39 000
Tampon phosphate (pH 7)	$6.5\times10^5 < K_d < 5\times10^{-6}$	28 000	22 000

Monomer extinction coefficient (ε_m), dimer extinction coefficient (ε_d) and dimerization constant (K_d).

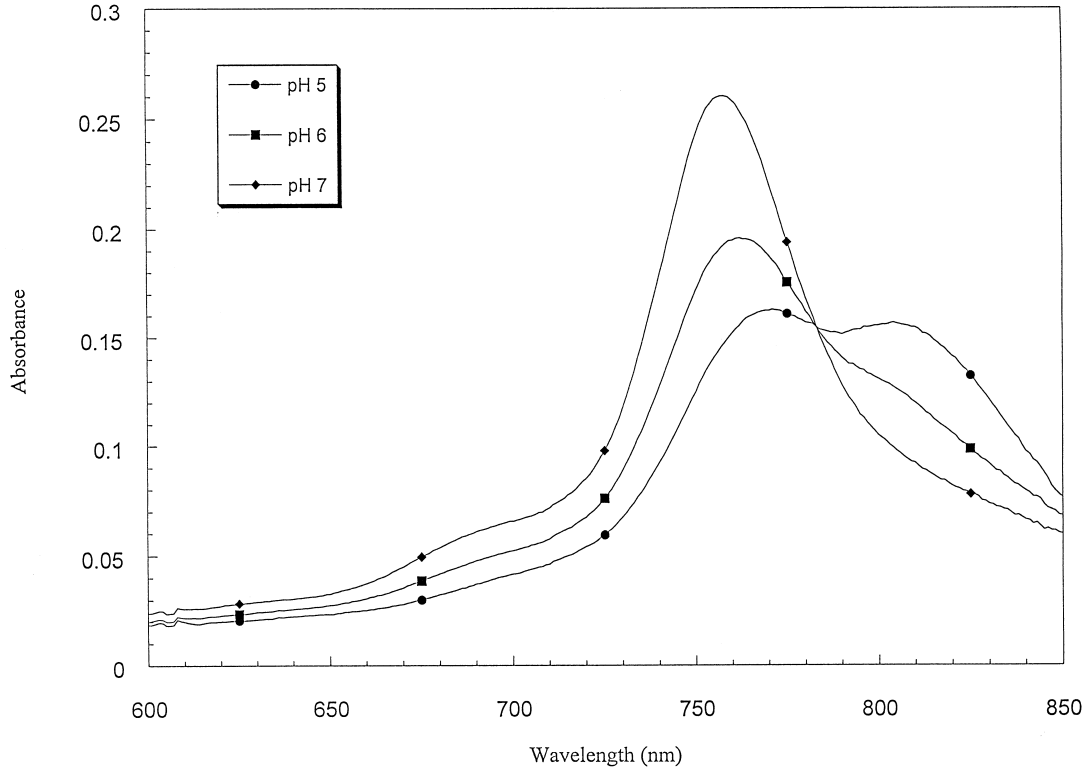

Fig. 6. pH dependence of the BCA (1.27×10^{-5} M) absorption spectrum in PBS. The spectra were recorded at 30 s after preparing the solution.

red shift of the peak at 760 nm towards 766 nm. Above 10^{-3} M lipids, no further shift was observed. In a vesicle suspension, in which all dye molecules are bound to the bilayers, any additional significant amount of BCA-unbound molecules must result in a spectrum which is the superposition of dye spectrum in water and dye spectrum in liposomes. For a ratio of concentration [BCA]/[DMPC] $>1:125$, the resulting experimental spectrum presented a shoulder in the band at 760 nm all the more important that the ratio was greater than 1:125. The spectrum obtained at [BCA]/[DMPC] smaller than 1:125 was similar to the BCA spectrum at the same concentration in methanol (Fig. 2).

Incorporation of BCA in liposomes caused an increase of the fluorescence intensity (peaks at ±770 and 670–680 nm) in comparison to its intensity in PBS. This increase was studied as a function of the lipid concentration at constant BCA concentration (1.2×10^{-5} M) in order to establish the ratio between dye and lipids at which all the BCA in suspension may be considered as bound to liposomes. When the total lipid concentration was increased above 1.5×10^{-3} M in the interval 1.5×10^{-4} to 2.5×10^{-3} M, the emission fluorescence reached a maximum (Fig. 7). The corresponding ratio between [BCA] and [DMPC] could be considered as the limit of incorporation of the dye.

3.3. Dependence of reduction rate on spin label localization

The fluorescence experiments presented in the previous section indicated that poorly water soluble BCA appeared to be completely bound to DMPC liposomes when the dye-to-lipids ratio was less than 1:125. In the present section, we present an ESR study of the solubilization depth of BCA within membrane. Under the condition [BCA]/[DMPC] $<1:125$, it was reasonable to suppose that 100% of the dye was taken up by the liposome.

The reduction of nitroxide spin labels, intercalated into BCA-treated DMPC liposomes or occupying the external aqueous phase, was measured by ESR upon irradiation with visible and UV light under anaerobic conditions, in order to investigate the location of the

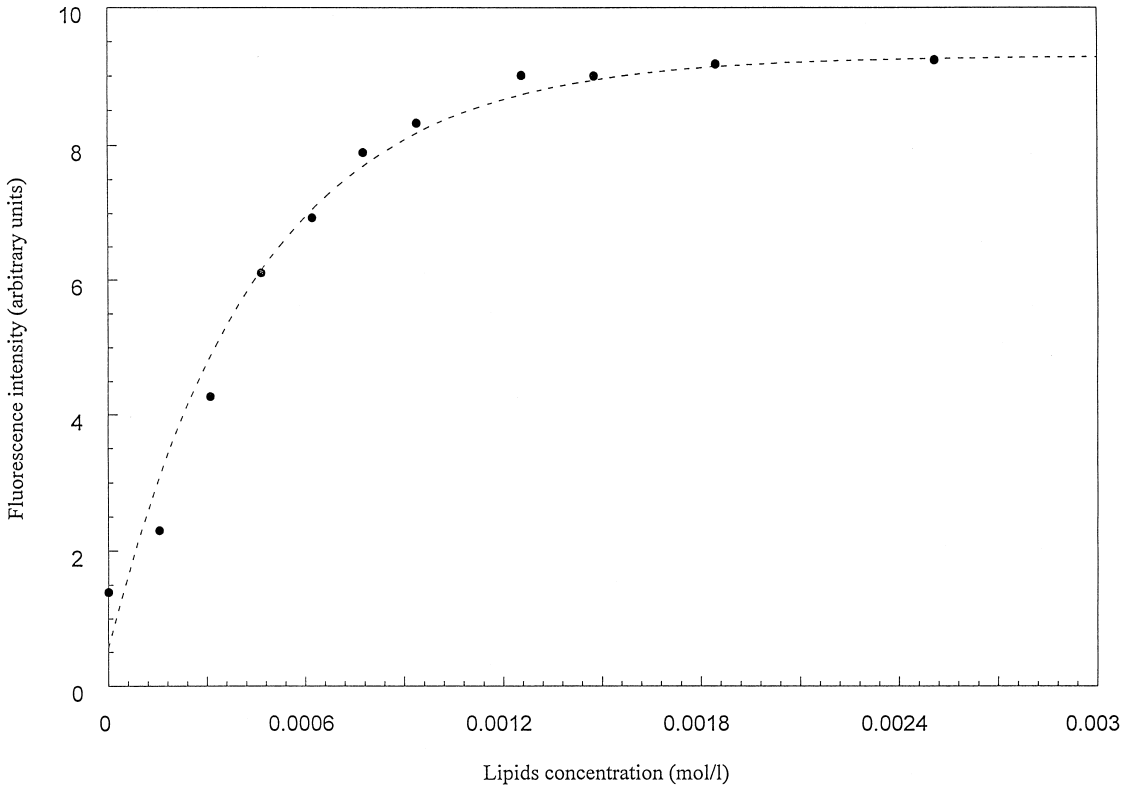

Fig. 7. Evolution of the emission fluorescence spectrum ($\lambda_{exc} = 355$ nm) of BCA (1.2×10^{-5} M) upon addition of DMPC vesicles in PBS, pH 7, at 25°C.

dye incorporated in the bilayer. In methanol, the ESR spectrum of the stearic acid spin probes (5-DSA, 12-DSA and 16-DSA) consisted of three symmetric absorption lines nearly indistinguishable from each which can be expected in a homogeneous solution. The incorporation into DMPC liposomes resulted in a change in the ESR spectrum of the label which is characteristic of strongly and weakly immobilized species (Fig. 8) without contribution of *n*-DSA present in the extra-liposomes' aqueous phase. The corresponding calculated order and correlation time parameters are in good agreement with previously published results [20,28–30]. The addition of BCA did not cause any change in the spectrum.

In homogeneous solvent, like N_2-saturated methanol, the series of *n*-DSA (2×10^{-5} M) studied were reduced at similar rates in the presence of photoexcited BCA (2×10^{-5} M). The reduction rate was linearly proportional to the BCA concentration and, in the absence of the dye or under O_2, no variation of the *n*-DSA signal amplitude was induced by irradiation of the sample (data not shown). On the other hand, the kinetics of signal amplitude reduction in BCA-treated DMPC liposomes were affected by the position of the doxyl moiety along the stearic acid chain. As shown in Fig. 9, the amount of 5-DSA whose doxyl moiety is close to the membrane surface decreased as a function of time whereas, the reduction of 12-DSA and 16-DSA whose doxyl moieties are deep in the membrane hydrocarbon region did not show any significant reduction. Fig. 9 also exhibits the reduction of the water soluble carbamoyl which kinetic was between those of 5-DSA and 12-DSA. In any case, the shape of the label ESR spectra was changed. In the absence of BCA or light or under O_2, no variation of the spin label concentration was observed in the liposome suspension.

Irradiated BCA was able to initiate a reduction of nitroxide occupying the external aqueous phase, while reduction of nitroxide embedded deeply in the hydrocarbon core were negligible. This result, together with the significant change in the 5-DSA concentration with time, suggest that the BCA solu-

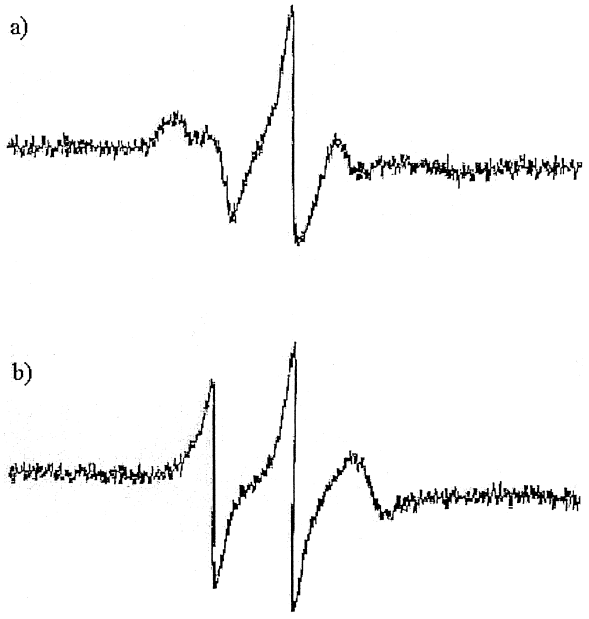

Fig. 8. ESR spectra of (a) 5-DSA and (b) 16-DSA in DMPC liposomes (20 mW microwave power, 1 G field modulation amplitude).

bilization site is located in the membrane bilayer at the outer surface.

By measuring the 5-DSA reduction rate when the concentration of BCA was increased at constant lipid concentration, it was also possible to check indirectly the limit of dye incorporation found by fluorescence technique. When the BCA concentration was increased from 7.5×10^{-6} to 5×10^{-5} M in the presence of DMPC (7.5×10^{-3} M) and 5-DSA (7.5×10^{-5} M), the spin label destruction rate increased until the ratio dye-to-lipid concentration reached 1:125. Above this limit, the reduction rates were essentially the same as shown on Fig. 10. This observation could indicate that under these experimental conditions, at least a portion of the BCA molecules resides in the aqueous phase and are not able to destroy the 5-DSA situated in the inner lipidic phase. This result would be consistent with the saturation limit obtained from the fluorescence data.

4. Discussion

The broadening and attenuation of the principal BCA absorption band, the apparition of shoulders and the presence in PBS of one isobestic point in the family of absorption curves were attributed to a monomer–dimer equilibrium. The deviation from Beer's law was particularly intense in water which is well known to be the most favorable solvent to

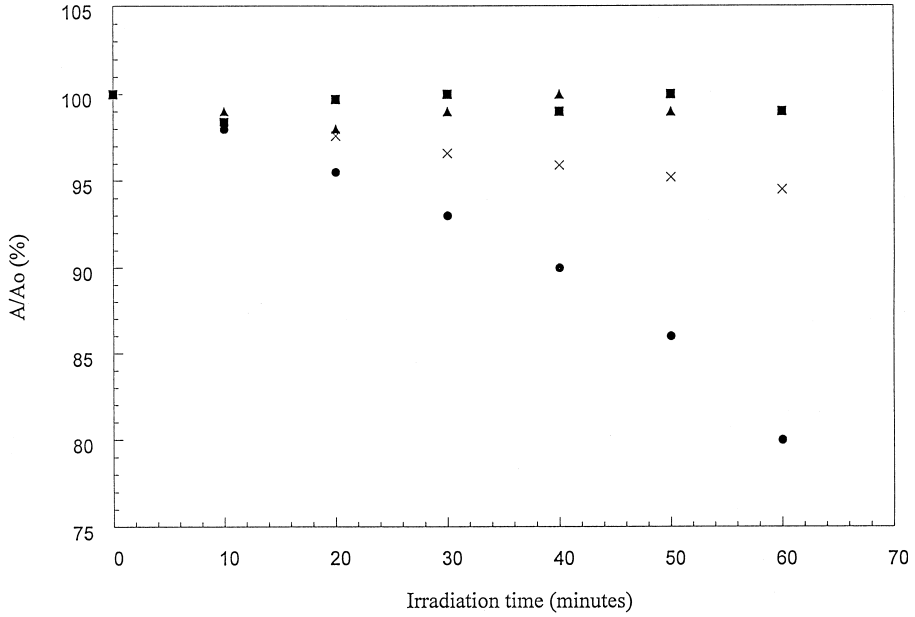

Fig. 9. BCA-mediated nitroxide reduction under anaerobic conditions. DMPC liposomes (7.4×10^{-3} M lipids) were treated with BCA (2×10^{-5} M). A/A_0 denotes the signal amplitude of nitroxide relative to the amplitude at time zero. ■, 16-DSA; ♦, 12-DSA; ×, CTPO; ●, 5-DSA.

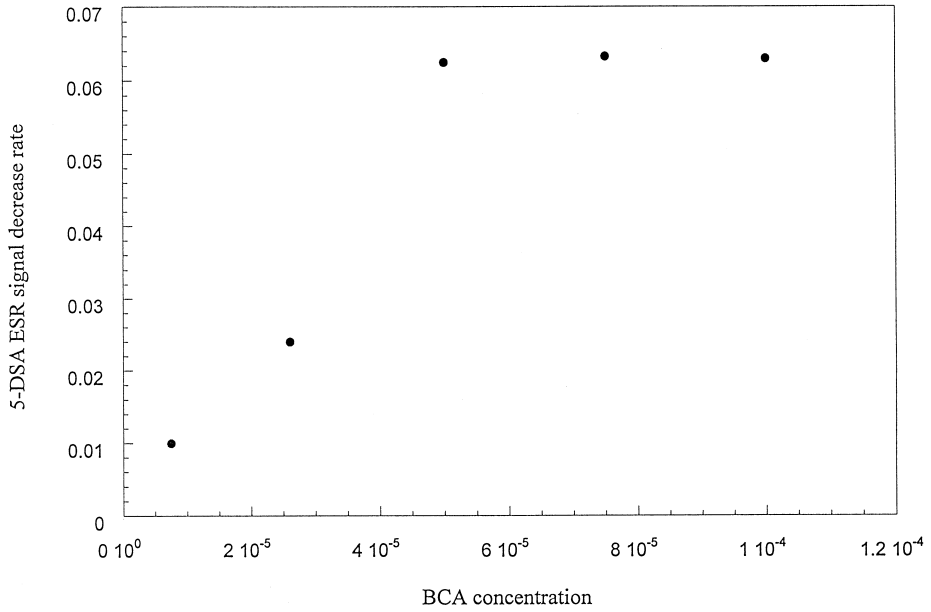

Fig. 10. 5-DSA (7.5×10^{-5} M) decrease rate as a function of BCA concentration in DMPC liposomes (7.5×10^{-3} M).

aggregation processes because of its very high dielectric constant [31,32]. Dimerization occurs at concentration as low as 10^{-6} M. The dye in methanolic solution is predominantly in monomeric form.

As shown in Fig. 6, a pH in the range 5–7 favors BCA aggregation process. The effect of lowered pH on the dye absorption properties is a well-known tendency of molecules with similar structures, their behavior in aqueous solutions being largely dominated by protonation and aggregation equilibria [33].

Among the various models which can be used to investigate the interactions of dye with membranes, liposomes are the most studied [34]. DMPC small unilamellar vesicles were chosen because this suitable system involves saturated lipids with a transition temperature of 23°C easily accessible. Two techniques were used to study the partition and the localization of BCA in liposomes: the monitoring of the dye fluorescence and absorption spectrum changes and the kinetic studies of spin label reductions.

BCA is incorporated into the lipid phase of DMPC liposomes in a monomeric state as indicated by the absence of spectral changes when dissolved in an organic solution or in an aqueous dispersion of DMPC liposomes at a dye-to-lipid ratio leading to complete dye binding. Like many other fluorescent dyes, the emission and absorption spectra of BCA are highly environment dependent [32,33,35]. Monomerization induced by dilution in liposomal suspension causes a red shift of the absorption maxima with a concomitant increase of the fluorescent emission. The DMPC liposome titration against a constant concentration of BCA results in a saturation curve of fluorescent enhancement. The BCA spectral behavior indicates that only at a lipid-to-dye ratio greater than 150 is a complete incorporation of the dye ensured.

Hydrophobic dyes like BCA to accumulate at different sites of the liposomal double membrane [16,36,37]. The kinetics of nitroxide spin labels were used to assess the dye localization in the biomembrane accurately. The control of such spatial distribution is very important for optimizing the efficiency of drug delivery from liposomes to cells [37].

As shown in Fig. 9, the DSA reduction rates are affected by the position of the doxyl moiety along the fatty acid chain. The more efficient quenching of 5-DSA, together with the absence of any significant reduction for 12-DSA and 16-DSA, are in favor of a localization of the dye near the polar head interface. Indeed, it is well established that the mean distance between the fatty acid carboxyl carbon and the carbon atom to which the doxyl group is bound is approximatively 8 Å [20]. 5-DSA explores the polar part of the liposome and its rate of reduction is controlled by the accessibility of the doxyl moieties to

the reducing agent, in that case, the excited BCA. Thus, the high rate of reduction obtained for 5-DSA suggests that BCA is located in the external surface of DMPC liposomes. Moreover, the observed reduction of the water soluble carbamoyl clearly indicates that at least a portion of BCA molecules resides close to the membrane surface.

The 5-DSA ESR signal decrease is also sensitive to BCA concentration at fixed lipid and spin label concentration (Fig. 10). Reduction rates increase with dye concentration in the range 7.5×10^{-6} to 5×10^{-5} M and they remain essentially the same above 5×10^{-5} M. Although above 5×10^{-5} M, dye and spin label concentrations are comparable, the concentration of excited state BCA is much less. Indeed, previous studies concerning bacteriochlorophyll derivatives have shown that the typical value for triplet quantum yield was estimated at 0.4 and our preliminary experimental data (data not shown) have indicated a value of 0.6 for BCA triplet quantum yield. Under those conditions, the step observed is not the consequence of an excess of dye in comparison with spin labels. The absence of any significant differences in the slopes at a dye-to-lipid ratio higher than 1:125 is not a surprising result with regard to our fluorescence data which suggest that 1:125 corresponds to the liposome limit of BCA incorporation. Since our ESR effects of the position of doxyl moiety on the rate of reduction of DSA show that BCA is located close to the polar liposome interface, the 5-DSA reduction rate dependence on BCA concentration confirms that the rates of reduction of DSA is controlled by the accessibility of the doxyl moiety to the dye. The limit step observed for the reduction of 5-DSA reflects that above 1:125, BCA is no more solubilized in the liposome, but in the aqueous phase where contact with 5-DSA becomes less efficient. The ESR quenching data fully support the fluorescence investigation. Moreover, they provide more detailed information on the BCA intraliposomal localization in unilamellar vesicles of DMPC.

Acknowledgements

M.H. is Senior Research Associate from Belgian National Fund for Scientific Research (NFSR, Brussels, Belgium). We acknowledge Dr. J. Den Hartigh and Ms. M.H. Langebroek from the department of Clinical Pharmacy and Toxicology of Leiden University Medical Center for HPLC measurements.

References

[1] M. Ochsner, Photophysical and photobiology processes in the photodynamic therapy of tumours, J. Photochem. Photobiol. Biol. 39 (1997) 1–18.
[2] M. Hoebeke, H. Schuitmaker, L. Jannink, M. Dubbelman, A. Jacobs, A. Van de Vorst, Electron spin resonance evidence of the generation of superoxide anion, hydroxyl radical and singlet oxygen during the photohemolysis of human erythrocytes with bacteriochlorin a, Photochem. Photobiol. 66 (1997) 502–508.
[3] J.J. Schuitmaker, J.A. Van Best, J.L. Van Delft, T.M.A.R. Dubbelman, J.A. Oosterhuis, D. de Wolff-Rouendull, Bacteriochlorin a, a new photosensitizer in photodynamic therapy: in vivo results, Invest. Ophthalmol. Vis. Sci. 31 (1990) 1444–1450.
[4] H.L.L.M. Van Leengoed, J.J. Schuitmaker, N. Van der Veen, T.M.A.R. Dubbelman, W.M. Star, Fluorescence and photodynamic effects of bacteriochlorin *a* observed in vivo in 'sandwich observation' chambers, Br. J. Cancer 67 (1993) 898–903.
[5] J.J. Schuitmaker, H.L.L.M. Van Leengoed, N. Van der Veen, T.M.A.R. Dubbelman, W.M. Star, Laser-induced in vivo fluorescence of bacteriochlorin *a*; preliminary results, Laser Med. Sci. 8 (1993) 39–42.
[6] I.P.J. Van Geel, H. Oppelaar, Y.G. Oussoren, J.J. Schuitmaker, F.A. Stewart, Mechanisms for optimizing PDT: second generation photosensitizers in combination with mitomycin C, Br. J. Cancer 72 (1995) 344–350.
[7] J.J. Schuitmaker, B.M. Koster, J.G.R. Elferink, The effects of photodynamic therapy on human neutrophil migration using bacteriochlorin *a*, Photochem. Photobiol. 68 (1998) 841–845.
[8] J.J. Schuitmaker, E.W. Vogel, J.F. Nagelkerke, R.P. Bos, Mutagenicity and dark toxicity of the second-generation photosensitizer bacteriochlorin *a*, J. Photochem. Photobiol. B. Biol. 47 (1998) 211–215.
[9] H.P. Van Iperen, H.J. Schuitmaker, G.M.J. Beijersbergen van Henegouwen, Non specific systemic immune suppression induced by photodynamic treatment of lymph node cells with bacteriochlorin *a*, J. Photochem. Photobiol. B: Biol. 28 (1995) 197–202.
[10] T.H. Foster, R.S. Murant, R.G. Bryant, R.S. Knox, S.L. Gibson, R. Hief, Oxygen consumption and diffusion effects in photodynamic therapy, Radiat. Res. 126 (1991) 296–303.
[11] J.P. Henning, R.L. Fourier, J.A. Hampton, A transient mathematical model of oxygen depletion during photodynamic therapy, Radiat. Res. 142 (1995) 221–226.
[12] A. Baker, J.R. Kanofsky, Quenching of singlet oxygen by

biomolecules from L1210 leukemia cells, Photochem. Photobiol. 55 (1992) 523–528.
[13] J.R. Kanofsky, Quenching of singlet oxygen by human red cell ghosts, Photochem. Photobiol. 53 (1991) 93–99.
[14] M. Ochsner-Bruderer, Zinc (II) – phthalocyanine, a photosensitizer for photodynamic therapy of tumours, Inaugural Dissertation, University of Basle, Basle, 1994.
[15] C.S. Foote, Type I and Type II mechanisms of photodynamic action, in: J.R. Heitz, K.R. Downum (Eds.), Light-Activated Pesticides, American Chemical Society, Washington, DC, 1987, pp. 22–38.
[16] F. Riccheli, G. Jori, S. Gobbo, M. Tronckin, Liposomes as models to study the distribution of porphyrins in cell membranes, Biochim. Biophys. Acta 1065 (1991) 42–48.
[17] A. Losi, Fluorescence and time-resolved photoacoustics of hypericin inserted in liposomes: dependence on pigment concentration and bilayer phase, Photochem. Photobiol. 65 (1997) 791–801.
[18] F. Riccheli, S. Gobbo, G. Jori, G. Moreno, F. Vinzens, C. Salet, Photosensitization of mitochondria by liposomes bound porphyrins, Photochem. Photobiol. 58 (1993) 53–58.
[19] L. Mayer, M. Hope, P. Cullis, Vesicles of variable sizes produced by rapid extrusion procedure, Biochim. Biophys. Acta 858 (1986) 161–168.
[20] M. Hoebeke, A. Seret, J. Piette, A. Van de Vorst, Destruction of stearic acid nitroxyl radicals mediated by photoexcited Merocyanine 540 in liposomal and micellar systems, Biochemistry 32 (1993) 2730–3736.
[21] W. West, S. Pearce, The dimeric state of cyanine dye, J. Phys. Chem. 69 (1965) 1894–1903.
[22] K. Sauer, J. Smith, A. Schultz, The dimerization of chlorophyll a, chlorophyll b and bacteriochlorophyll in solution, J. Am. Chem. Soc. 88 (1996) 2681–2688.
[23] D. Brault, C. Vever-Bizet, T. Le Doan, Spectrofluorimetric study of porphyrin incorporation into membrane models – evidence for pH effects, Biochim. Biophys. Acta 857 (1986) 238–250.
[24] L. Sikurova, I. Haban, D. Chorvat, Dimers of merocyanine 540, I. In aqueous solutions, Stud. Biophys. 125 (1988) 197–201.
[25] L. Sikura, I. Haban, R. Frankova, Dimers of merocyanine 540, II. In egg lecithin liposomes, Stud. Biophys. 128 (1988) 103–108.
[26] L. Sikura, R. Frankova, D. Chorvat, Dimers of merocyanine 540, III. In dimyristoyl lecithin liposomes, Stud. Biophys. 133 (1989) 67–72.
[27] B. Ehrenberg, E. Pevzner, Spectroscopic properties of the potentiometric probe merocyanine 540 in solutions and in liposomes, Photochem. Photobiol. 57 (1993) 228–234.
[28] K. Chen, P. Morse II, M. Swartz, Kinetics of enzyme-mediated reduction of lipid soluble nitroxide spin labels by living cells, Biochim. Biophys. Acta 943 (1988) 477–484.
[29] M. Takahashi, J. Tsuchiya, E. Niki, S. Urano, Action of vitamin E as antioxidant in phospholipid liposomal membranes as studied by spin label technique, J. Nutr. Sci. Vitaminol. 34 (1988) 25–34.
[30] J. Feix, B. Kalyanaraman, An electron spin resonance study of merocyanine 540- mediated type I reactions in liposomes, Photochem. Photobiol. 53 (1991) 39–45.
[31] R. Bensasson, E. Land, T. Truscott, Flash Photolysis and Pulse Radiolysis, Pergamon Press, Oxford, 1983, pp. 20–66.
[32] C. Balny, S. Seymour, G. Hui Bon Hoa, Absorption and fluorescence spectra of chlorophyll-a in polar solvents as a function of temperature, Photochem. Photobiol. 9 (1969) 445–454.
[33] D. Brault, Physical chemistry of porphyrins and their interactions with membranes: the importance of pH, J. Photochem. Photobiol. B: Biol. 6 (1990) 79–86.
[34] D. Brault, C. Vever-Bizet, K. Kuzelova, Interactions of dicarboxylic porphyrins with membranes in relation to their ionization state, J. Photochem. Photobiol. B: Biol. 20 (1993) 191–195.
[35] J. Connolly, E. Samuel, F. Janzen, Effect of solvent on the fluorescence properties of bacteriochlorophyll a, Photochem. Photobiol. 36 (1982) 565–574.
[36] F. Richelli, G. Jori, Distribution of porphyrins in the various compartments of unilamellar liposomes of dipalmitoyl-phosphatidylcholine as probed by fluorescence spectroscopy, Photochem. Photobiol. 44 (1986) 151–157.
[37] H. Toledano, R. Edrei, S. Kimel, Photodynamic damage by liposome-bound porphycenes: comparison between in vitro and in vivo models, J. Photochem. Photobiol. B: Biol. 42 (1998) 20–27.